Multifunctional Eu(III) Modified HOFs: Roxarsone and Aristolochic Acid Carcinogen Monitoring and Latent Fingerprint Identification Based on Artificial Intelligence

Kai Zhu,[a] and Bing Yan*,[a]

[a] *Shanghai Key Lab of Chemical Assessment and Sustainability, School of Chemical Science and Engineering, Tongji University, Siping Road 1239, Shanghai 200092, China. E-mail: byan@tongji.edu.cn.*

Electronic supplementary information

Materials and physical measurements

Figure S16. The deviation curve of SVM. [Node Number: the number of input layer, Q: Quenched (0), U: Unchanged (1).]

Figure S17. (a) Emission spectra (λ_{ex} = 324 nm) of Eu@**1** in various concentrations of Rox solution (2×10^{-5} - 1×10^{-3} M). (b) Dependence of the emission intensity of $^5D_0\rightarrow{}^7F_2$ (614 nm) on $\log C_{Rox}$ (2×10^{-5} - 1×10^{-3} M).

Figure S18. Photo of Eu@**1** after immersed into various concentrations of Rox solutions (5×10^{-5} - 1×10^{-3} M) under 310 nm UV-light irradiation.

Figure S19. (a) Fluorescence spectra of Eu@**1** in 10^{-3} M different chicken and egg-white specie solutions. (b) The histogram of emission intensities at 614 nm ($^5D_0\rightarrow{}^7F_2$) of Eu@**1** dispersed in different solutions of common chicken and egg-white species.

Figure S20. (a) The histogram of relative intensities of luminescence response of Eu@**1** at 614 nm ($^5D_0\rightarrow{}^7F_2$) toward Rox in the presence of other common chicken and egg-white components.

Figure S21. Photo of Eu@**1** after immersed into various concentrations of AA solutions (1×10^{-3} - 1×10^{-6} M) under 310 nm UV-light irradiation.

Figure S22. (a) Dependence of the emission intensity of $^5D_0\rightarrow{}^7F_2$ (614 nm) on $\log C_{AA}$ (1×10^{-6} - 1×10^{-3} M). (b) Luminescence intensity of 614 nm peak for Eu@**1** after five repetitions with 10^{-3} M AA solution.

Figure S23. (a) Kinetic-time scanning spectroscopy at 614 nm of Eu@**1** upon addition of 10^{-3} M AA. (b) Fluorescence spectra of Eu@**1** in 10^{-3} M different serum specie solutions.

Figure S24. (a) The histogram of relative intensities of luminescence response of Eu@**1** at 614 nm ($^5D_0\rightarrow{}^7F_2$) toward AA in the presence of other serum components. (b) The histogram of emission intensities at 614 nm ($^5D_0\rightarrow{}^7F_2$) of Eu@**1** dispersed in different solutions of common serum species.

Figure S25. PXRD patterns of Eu@**1** before and after immersing into Rox and AA suspensions.

Figure S26. (a) UV-vis absorption spectra and excitation spectrum of (a) Rox and Eu@**1**, (b) AA and Eu@**1**.

Figure S27. Excitation spectra of Eu@**1** under different concentrations of Rox (0 - 1×10^{-3} M).

Figure S28. (a) Excitation spectra of Eu@**1** under different concentrations of AA (0 - 5×10^{-4} M)**.** (b) emission spectra of Eu@**1** under different concentrations of AA (0 - 5×10^{-4} M).

Figure S29. Decay lifetimes of emission peak of 614 nm ($^5D_0\rightarrow{}^7F_2$ transition) for Eu@**1** with a series of concentrations of (a) Rox and (b) AA.

Figure S30. Energy level diagram indicating the quenched sensing mechanism of Eu@**1** to Rox and AA. (ISC: intersystem crossing).

Figure S31. Emission spectra of Eu@**1** in various concentrations of (a) Rox in chicken extracting solution (8×10^{-5} - 1×10^{-3} M), (c) Rox in egg-white extracting solution (8×10^{-5} - 1×10^{-3} M) and (e) AA in serum solution (1×10^{-5} - 1×10^{-3} M). Calibration curves of Eu@**1** toward (b) Rox in chicken extracting solution (8×10^{-5} - 1×10^{-3} M), (d) Rox in egg-white extracting solution (8×10^{-5} - 1×10^{-3} M) and (f) AA in serum (1×10^{-5} - 1×10^{-3} M).

Figure S32. The fingerprint images developed by Eu@**1** from the right hand of volunteer 1 (suspect 1) in the fingerprint database used for training in Alexnet: (a) Ten thumbprint images. (b) Ten index finger fingerprint images. (c) Ten middle finger fingerprint images. (d) Ten ring finger fingerprint images. (e) Ten little finger fingerprint images.

Figure S33. The fingerprint images developed by Eu@**1** from the right hand of volunteer 2 (suspect 2) in the fingerprint database used for training in Alexnet: (a) Ten thumbprint images. (b)

Ten index finger fingerprint images. (c) Ten middle finger fingerprint images. (d) Ten ring finger fingerprint images. (e) Ten little finger fingerprint images.

Figure S34. The fingerprint images developed by Eu@**1** from the right hand of volunteer 3 (suspect 3) in the fingerprint database used for training in Alexnet: (a) Ten thumbprint images. (b) Ten index finger fingerprint images. (c) Ten middle finger fingerprint images. (d) Ten ring finger fingerprint images. (e) Ten little finger fingerprint images.

Figure S35. The fingerprint images developed by Eu@**1** from the right hand of volunteer 4 (suspect 4) in the fingerprint database used for training in Alexnet: (a) Ten thumbprint images. (b) Ten index finger fingerprint images. (c) Ten middle finger fingerprint images. (d) Ten ring finger fingerprint images. (e) Ten little finger fingerprint images.

Figure S36. The fingerprint images developed by Eu@**1** from the right hand of volunteer 5 (suspect 5) in the fingerprint database used for training in Alexnet: (a) Ten thumbprint images. (b) Ten index finger fingerprint images. (c) Ten middle finger fingerprint images. (d) Ten ring finger fingerprint images. (e) Ten little finger fingerprint images.

Figure S37. (a) Accuracy training curve of Alexnet neural network after 1400 iterations. (b) Loss training curve of Alexnet neural network after 1400 iterations.

Table S1. Element contents of C and O in EDX energy spectrum of **1** and C, O and Eu in EDS energy spectrum of Eu@**1**.

Table S2. Summary of fluorescence decay lifetime for Eu@**1** powder, Eu@**1** in 90% ethanol, Eu@**1** with 1×10^{-4} M - 5×10^{-4} M Rox, Eu@**1** with 1×10^{-4} M - 5×10^{-4} M AA.

Table S3. Summary of S_1 and T_1 energy levels (eV) of tcpb calculated by the time dependent density functional theory (TD-DFT) method.

Table S4. Summary of excitation and emission transitions, and experimental energy gaps of tcpb, HOF-BTB and Eu^{3+}.

Table S5. Summary of input and output information during the training for SVM.

Table S6. Training result information for SVM.

Table S7. The value deviation table for SVM.

Table S8. The MATLAB code of the SVM.

Table S9. Summary of fluorescence sensing parameters of Eu@**1** for detecting Rox, AA, Rox in chicken, Rox in egg-white, and AA in serum.

Table S10. Comparison of the proposed method in this work with some previously similar reported methods for Rox and AA detection.

Table S11. The MATLAB code of AFIS.

Table S12. The MATLAB code of AlexNet-FAP.

Materials and physical measurements

$Eu@(NO_3)_3·6H_2O$ was prepared by dissolving their oxides in excess hydrogen nitrate with continuous stirring, followed by evaporation and crystallization several times. All the other reagents and solvents employed were commercially available and used as received without further purification. The goat serum was purchased from Shenggong Bioengineering (Shanghai) Co., Ltd. Ultrapure water was used throughout all experiments. The power X-ray diffraction (PXRD) pattern was recorded via a Bruker D8 Advance diffractometer, with a scan range of 2 theta from 5° to 50°. Fourier transform infrared spectra (FT-IR) of powder samples were collected on a Nicolet IS10 infrared spectrum radiometer in the range of 4000 - 400 cm^{-1} using KBr slices. Thermal gravimetric analysis (TGA) was carried out on a Netzsch STA 449C system at a heating rate of 5 K min^{-1} from 40 ℃ temperature to 800 ℃ under nitrogen atmosphere in the Al_2O_3 crucibles. Scanning electron microscopy (SEM) and energy dispersive X-ray (EDX) analysis were performed on a Hitachi S-4800 field emission scanning electron microscope operating at 3 KV and 15 KV, respectively. X-ray photoelectron spectroscopy (XPS) spectra were recorded under ultrahigh vacuum ($<10^{-6}$ Pa) at a pass energy of 93.90 eV with an Axis Ultra DLD spectrometer (Kratos, Japan) by using an Mg Kα (1253.6 eV) anode. Nitrogen adsorption/desorption isotherms were measured by a Tristar 2460 analyzer at the liquid nitrogen temperature. The samples were outgassed at 130 °C for 6 h before the measurements. The Brunauer Emmett Teller (BET) method was used to calculate the surface area from the adsorption data. The excitation and emission spectra of the experimental samples were obtained on an Edinburgh FLS920 spectrophotometer with a xenon lamp (450 W) as an excitation source. Luminescence lifetime measurements were measured at room temperature on an Edinburgh FLS920 phosphorimeter using a microsecond lamp (100 mW). The corresponding Commission International de l'Eclairage (CIE) color coordinates were calculated based on CIE 1931 constructed by Orign 2023 program. The PCA and HCA was constructed in Origin 2023. The SVM model was constructed in Maishi Support Vector Machine. The AFIS and Alexnet-FAP were conducted by MATLAB 2023.

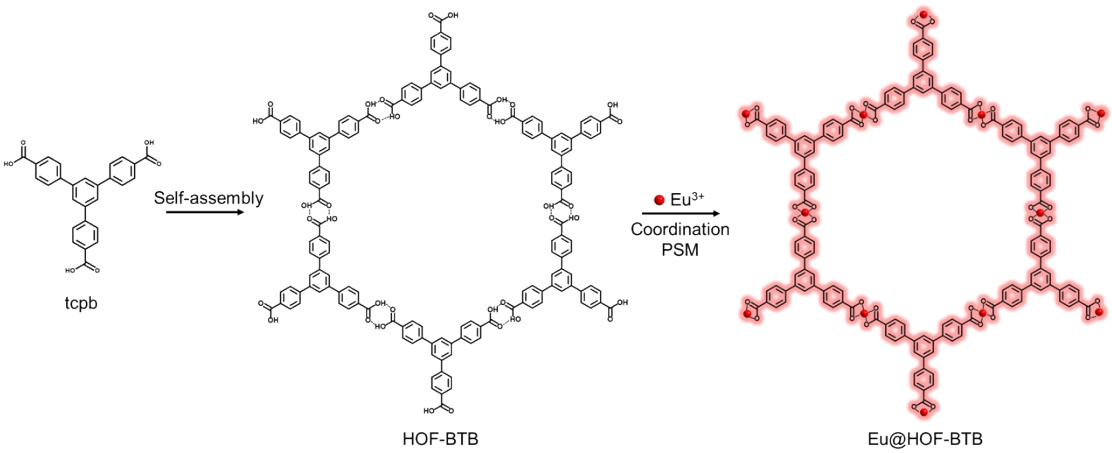

Figure S1. The graphical illustration of the synthesis of HOF-BTB (**1**) and Eu@HOF-BTB (Eu@**1**).

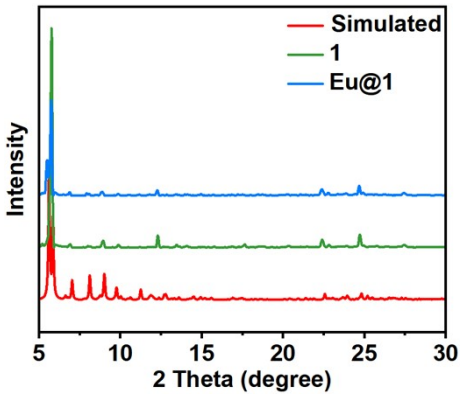

Figure S2. Experimental PXRD patterns from 5° to 30° of **1** and Eu@**1**.

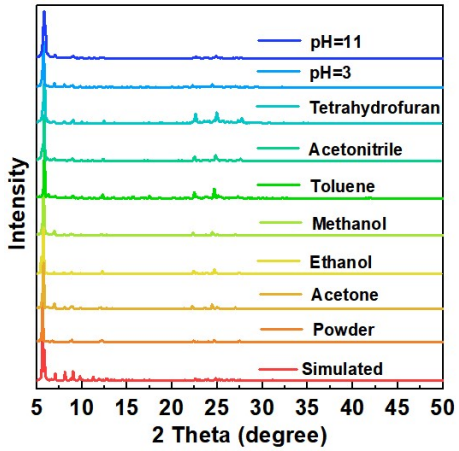

Figure S3. PXRD patterns of Eu@**1** powder and Eu@**1** taken out from acetone, ethanol, methanol, toluene, acetonitrile, trichloromethane, acidic (pH = 3), and alkaline (pH = 11) aqueous solutions.

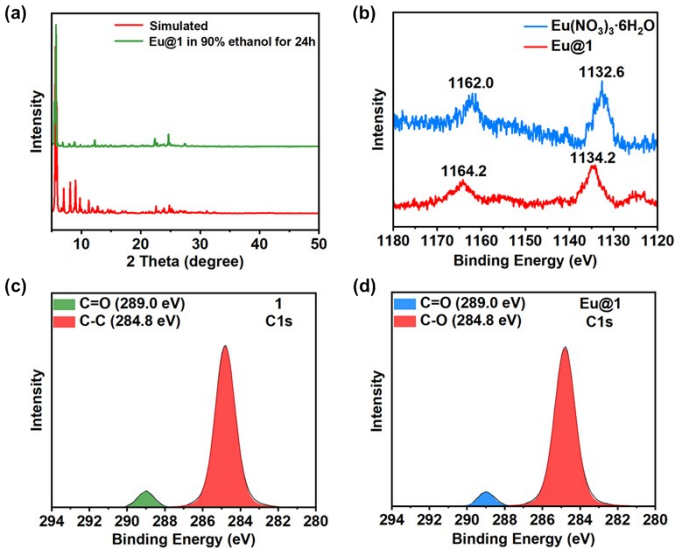

Figure S4. (a) PXRD pattern of Eu@**1** after immersed in 90% ethanol (ethanol: water = 9:1) solvent for 24 h. (b) XPS spectra of Eu 3d electron in $Eu(NO_3)_3·6H_2O$ (blue line) and Eu 3d electron in Eu@**1** (red line). XPS spectra of (c) C 1s electron in **1**, (d) C 1s electron in Eu@**1**.

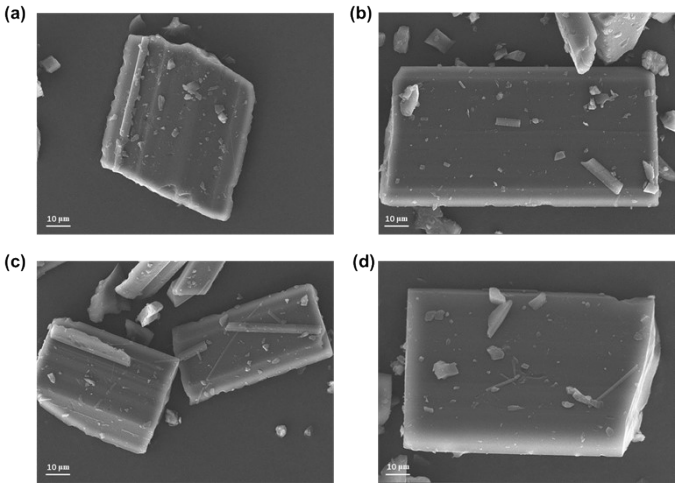

Figure S5. (a) (b) (c) (d) SEM picture of **1**.

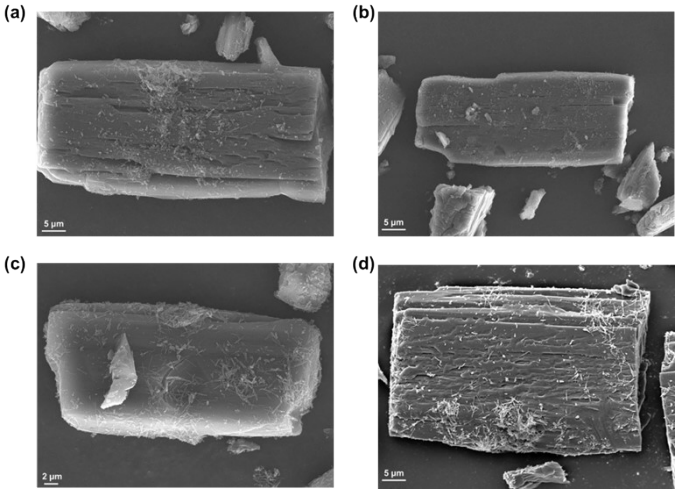

Figure S6. (a) (b) (c) (d) SEM picture of Eu@**1**.

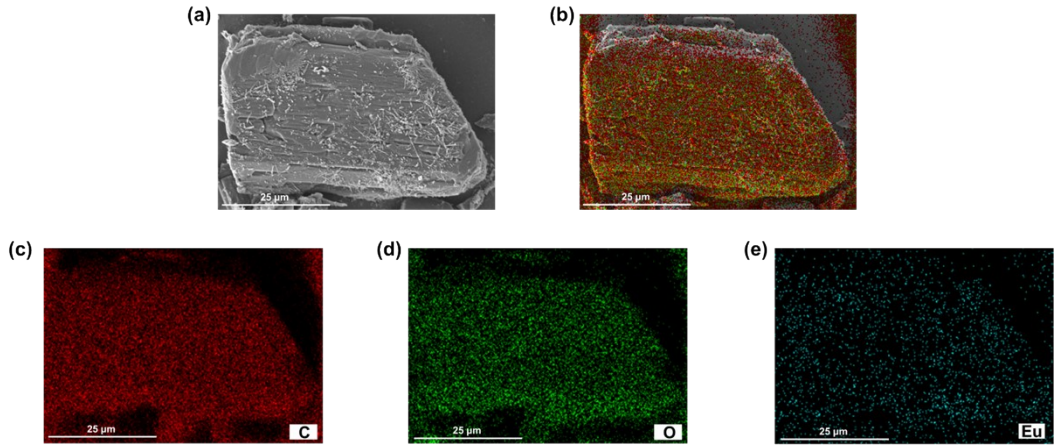

Figure S7. (a) SEM picture of Eu@**1**. (b) EDS layered image of Eu@**1**. (c) (d) (e) EDS mapping images of C, O and Eu elements in Eu@**1**, respectively.

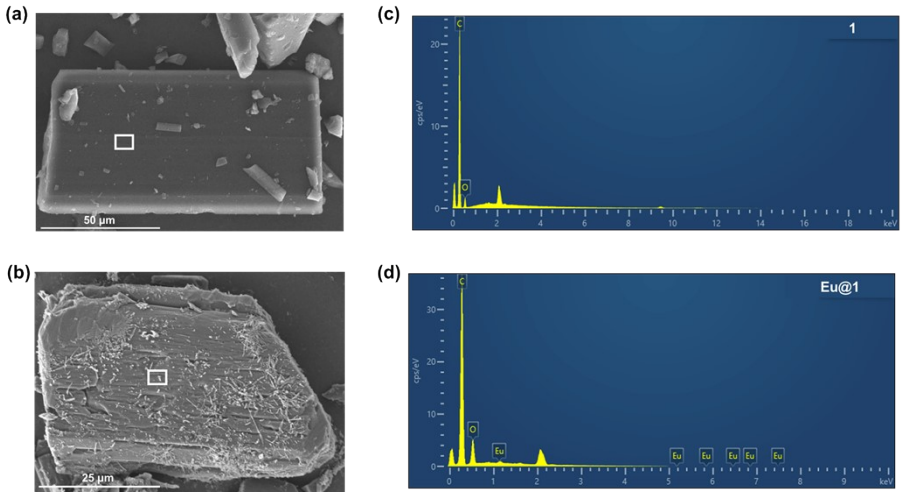

Figure S8. SEM image of (a) **1** and (b) Eu@**1**. (c) The weight content of C (90.54%) and O (9.46%) elements in EDS energy spectrum of **1**. (d) The weight content of C (85.36%), O (9.07%) and Eu (5.57%) elements in EDS energy spectrum of Eu@**1**.

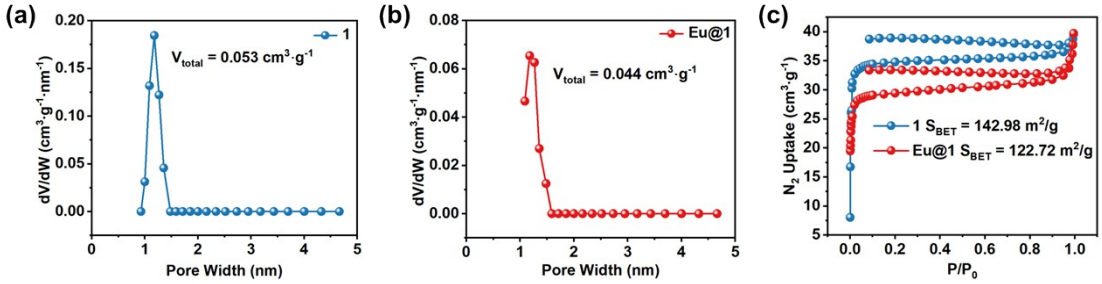

Figure S9. Pore size distributions of (a) **1**, and (b) Eu@**1**. (c) N_2 adsorption/desorption isotherms of **1** and Eu@**1**. (V = pore volume)

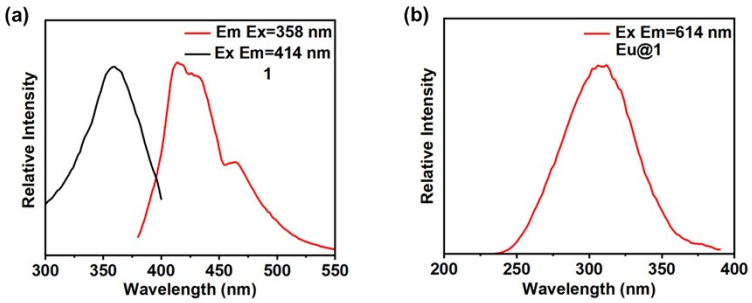

Figure S10 (a) Excitation and Emission spectrum of **1**. (b) Excitation spectrum of Eu@**1**.

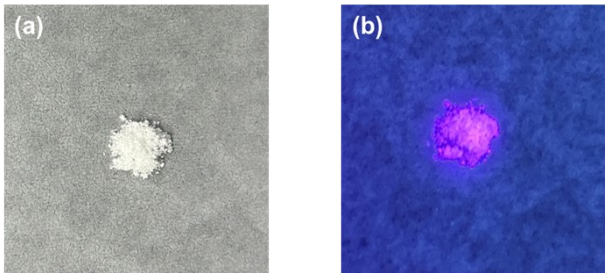

Figure S11. The photographs of Eu@**1** powder in solid state (a) under normal light. (b) after excitation under a 310 nm UV lamp.

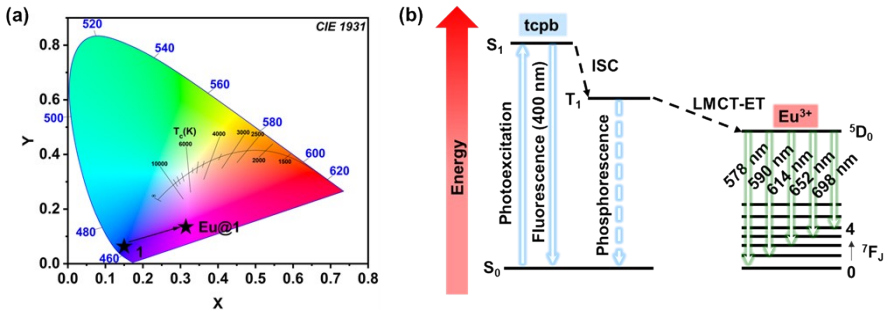

Figure S12. (a) CIE chromaticity coordinates of **1** powder (0.1499, 0.0629) and Eu@**1** powder (0.3145, 0.1342). (b) Schematic diagram for LMCT-ET progress for Eu@**1** (ISC: intersystem crossing; ET: energy transfer; LMCT: ligand-to-metal charge transfer).

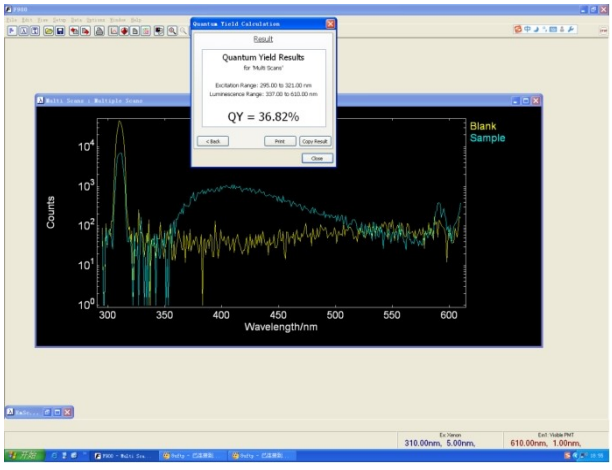

Figure S13. Photoluminescence quantum yield (PLQY) of Eu@**1**.

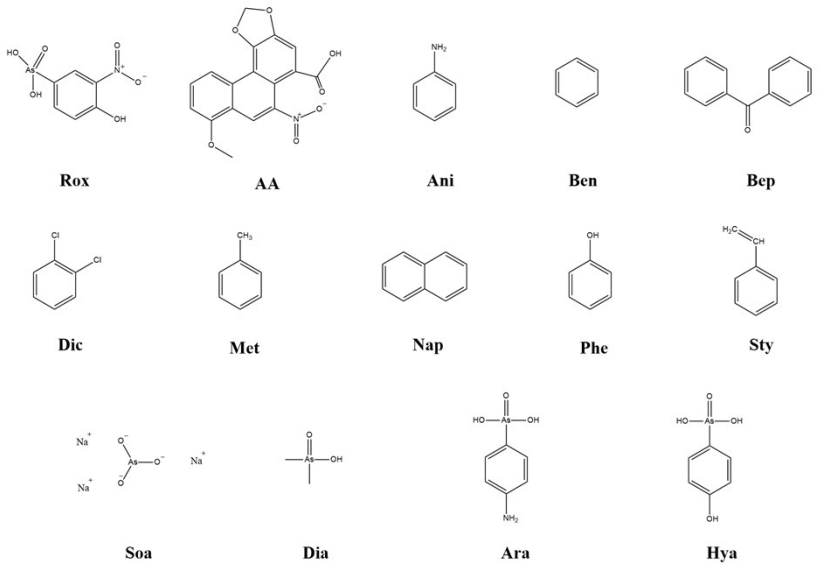

Figure S14. The chemical diagrams of the aromatic and arsenic-containing carcinogens including roxarsone (Rox), aristolochic acid (AA), aniline (Ani), benzene (Ben), Benzophenone (Bep), Dichlorobenzene (Dic), Methylbenzene (Met), Naphthalene (Nap), Phenol (Phe), Styrene (Sty), sodium Arsenite (Soa), dimethylarsinic acid (Dia), P-arsanilic acid (arsanilic acid, Ara) and 4-hydroxyphenylarsonic acid (Hya).

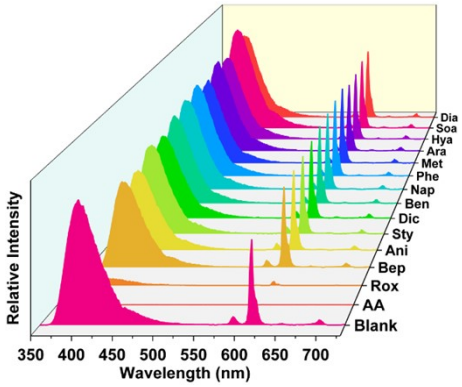

Figure S15. Fluorescence spectra of Eu@**1** in 10^{-3} M different aromatic and arsenide-containing carcinogen solutions.

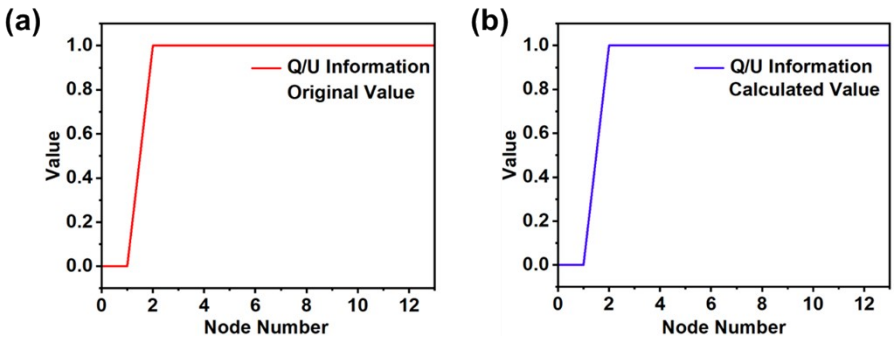

Figure S16. The deviation curve of SVM. [Node Number: the number of input layer, Q: Quenched (0), U: Unchanged (1).]

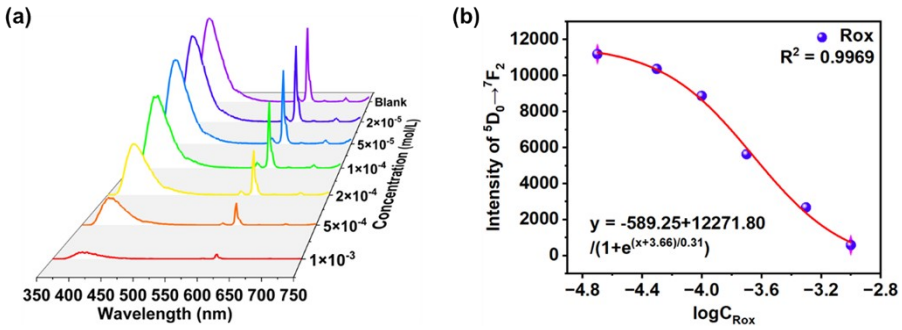

Figure S17. (a) Emission spectra (λ_{ex} = 324 nm) of Eu@**1** in various concentrations of Rox solution (2×10^{-5} - 1×10^{-3} M). (b) Dependence of the emission intensity of $^5D_0\rightarrow{}^7F_2$ (614 nm) on $logC_{Rox}$ (2×10^{-5} - 1×10^{-3} M).

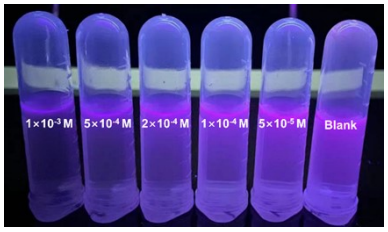

Figure S18. Photo of Eu@**1** after immersed into various concentrations of Rox solutions (5×10^{-5} - 1×10^{-3} M) under 310 nm UV-light irradiation.

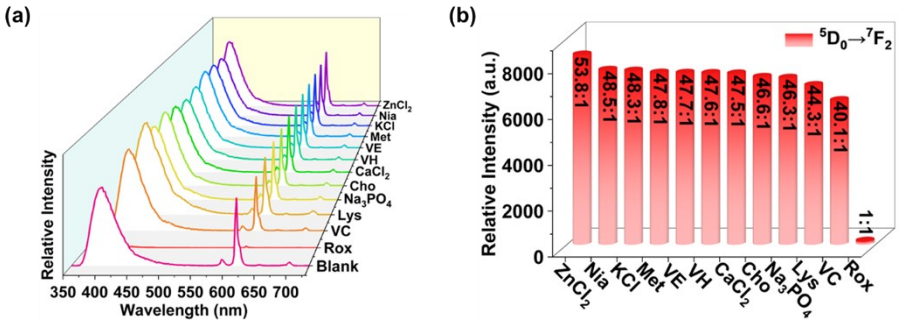

Figure S19. (a) Fluorescence spectra of Eu@**1** in 10^{-3} M different chicken and egg-white specie solutions. (b) The histogram of emission intensities at 614 nm ($^5D_0\rightarrow{}^7F_2$) of Eu@**1** dispersed in different solutions of common chicken and egg-white species.

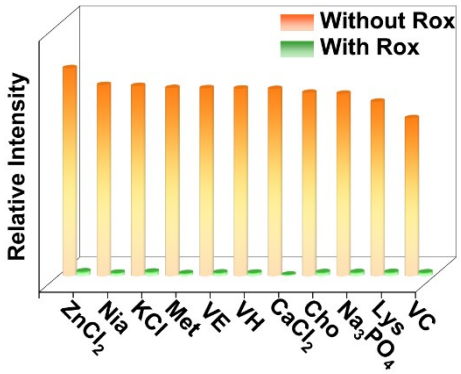

Figure S20. (a) The histogram of relative intensities of luminescence response of Eu@**1** at 614 nm ($^5D_0\rightarrow{}^7F_2$) toward Rox in the presence of other common chicken and egg-white components.

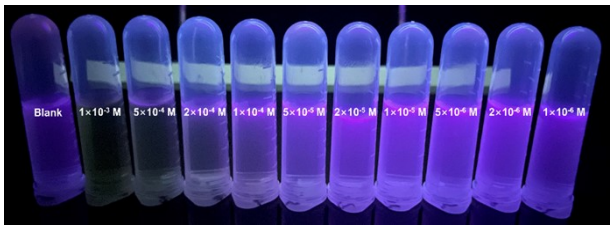

Figure S21. Photo of Eu@**1** after immersed into various concentrations of AA solutions (1×10^{-3} - 1×10^{-6} M) under 310 nm UV-light irradiation.

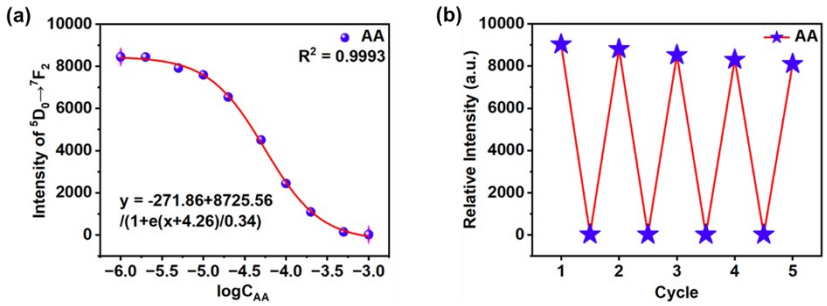

Figure S22. (a) Dependence of the emission intensity of $^5D_0\rightarrow{}^7F_2$ (614 nm) on $\log C_{AA}$ (1×10^{-6} - 1×10^{-3} M). (b) Luminescence intensity of 614 nm peak for Eu@**1** after five repetitions with 10^{-3} M AA solution.

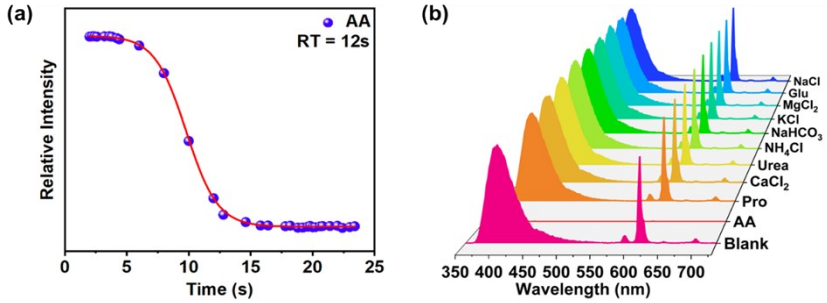

Figure S23. (a) Kinetic-time scanning spectroscopy at 614 nm of Eu@**1** upon addition of 10^{-3} M AA. (b) Fluorescence spectra of Eu@**1** in 10^{-3} M different serum specie solutions.

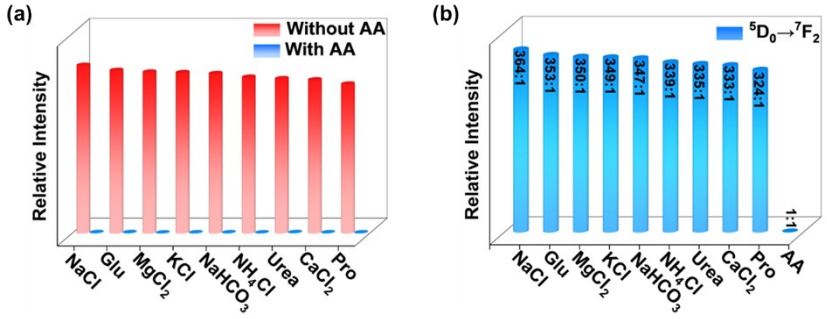

Figure S24. (a) The histogram of relative intensities of luminescence response of Eu@**1** at 614 nm ($^5D_0\rightarrow{}^7F_2$) toward AA in the presence of other serum components. (b) The histogram of emission intensities at 614 nm ($^5D_0\rightarrow{}^7F_2$) of Eu@**1** dispersed in different solutions of common serum species.

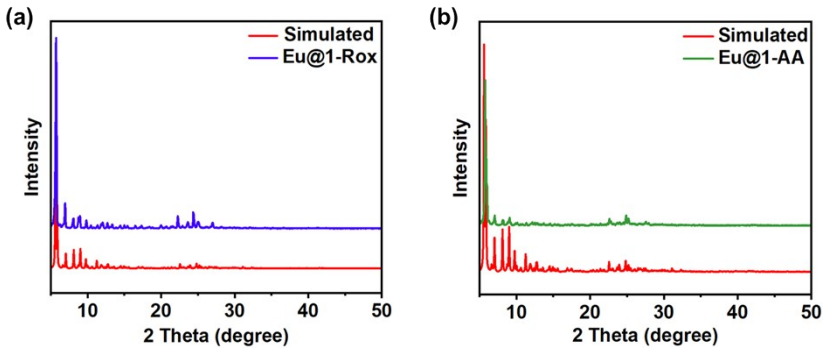

Figure S25. PXRD patterns of Eu@**1** before and after immersing into Rox and AA suspensions.

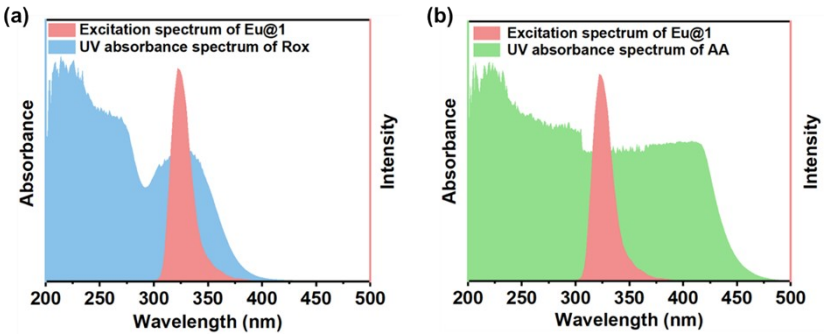

Figure S26. (a) UV-vis absorption spectra and excitation spectrum of (a) Rox and Eu@**1**, (b) AA and Eu@**1**.

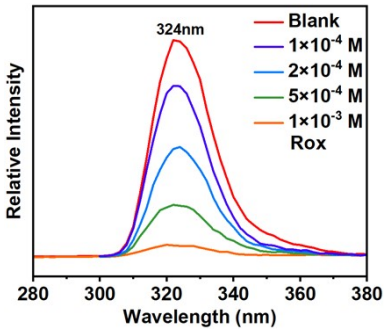

Figure S27. Excitation spectra of Eu@**1** under different concentrations of Rox (0 - 1×10^{-3} M).

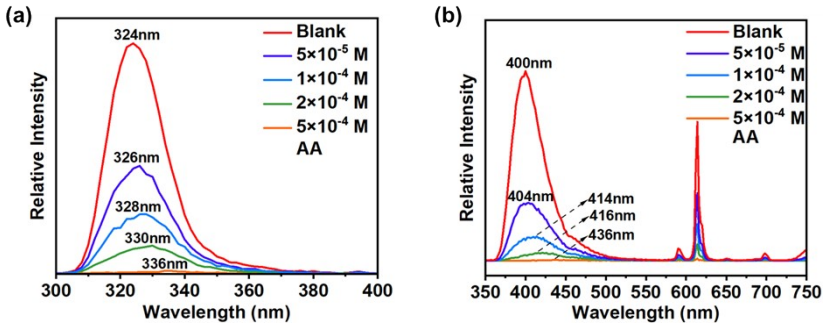

Figure S28. (a) Excitation spectra of Eu@**1** under different concentrations of AA (0 - 5×10^{-4} M)**.** (b) emission spectra of Eu@**1** under different concentrations of AA (0 - 5×10^{-4} M).

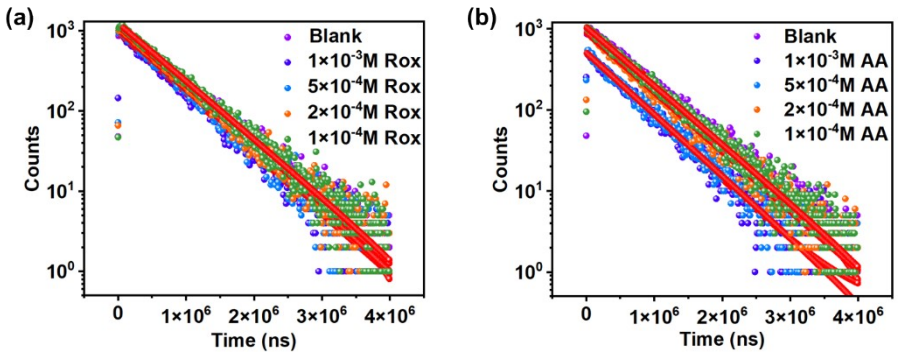

Figure S29. Decay lifetimes of emission peak of 614 nm ($^5D_0 \rightarrow {}^7F_2$ transition) for Eu@**1** with a series of concentrations of (a) Rox and (b) AA.

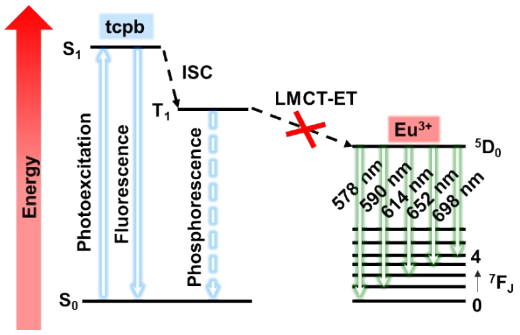

Figure S30. Energy level diagram indicating the quenched sensing mechanism of Eu@**1** to Rox and AA. (ISC: intersystem crossing).

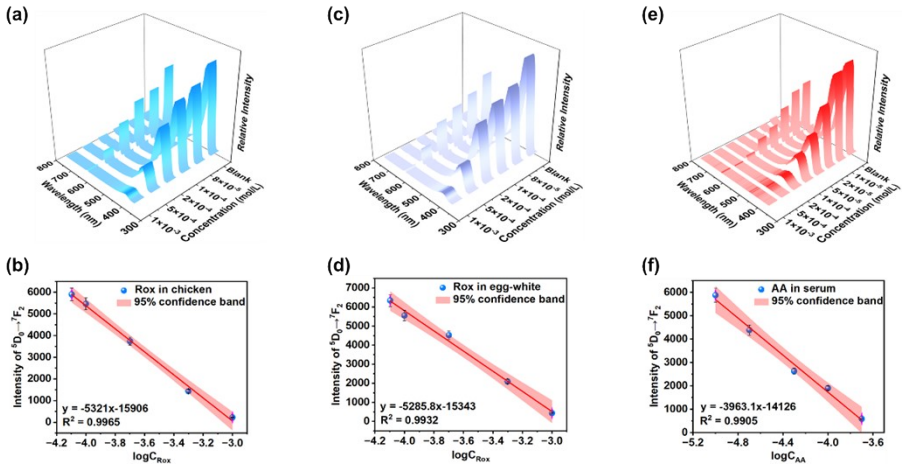

Figure S31. Emission spectra of Eu@**1** in various concentrations of (a) Rox in chicken extracting solution (8×10^{-5} - 1×10^{-3} M), (c) Rox in egg-white extracting solution (8×10^{-5} - 1×10^{-3} M) and (e) AA in serum solution (1×10^{-5} - 1×10^{-3} M). Calibration curves of Eu@**1** toward (b) Rox in chicken extracting solution (8×10^{-5} - 1×10^{-3} M), (d) Rox in egg-white extracting solution (8×10^{-5} - 1×10^{-3} M) and (f) AA in serum (1×10^{-5} - 1×10^{-3} M).

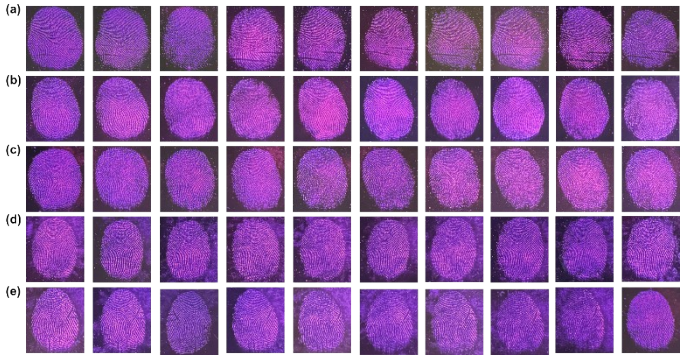

Figure S32. The fingerprint images developed by Eu@**1** from the right hand of volunteer 1 (suspect 1) in the fingerprint database used for training in Alexnet: (a) Ten thumbprint images. (b) Ten index finger fingerprint images. (c) Ten middle finger fingerprint images. (d) Ten ring finger fingerprint images. (e) Ten little finger fingerprint images.

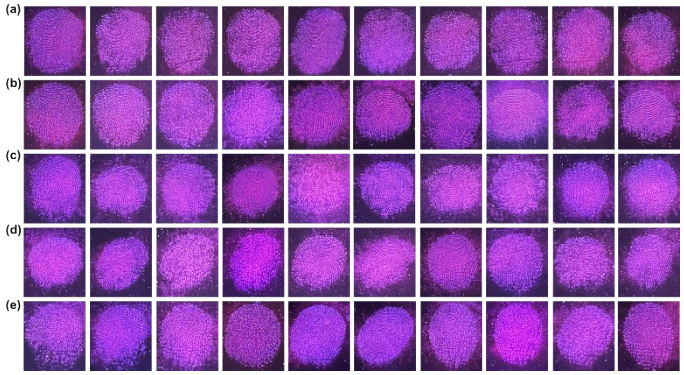

Figure S33. The fingerprint images developed by Eu@**1** from the right hand of volunteer 2 (suspect 2) in the fingerprint database used for training in Alexnet: (a) Ten thumbprint images. (b) Ten index finger fingerprint images. (c) Ten middle finger fingerprint images. (d) Ten ring finger fingerprint images. (e) Ten little finger fingerprint images.

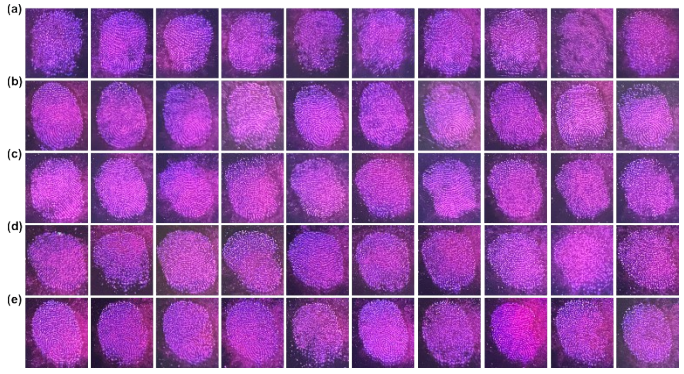

Figure S34. The fingerprint images developed by Eu@**1** from the right hand of volunteer 3 (suspect 3) in the fingerprint database used for training in Alexnet: (a) Ten thumbprint images. (b) Ten index finger fingerprint images. (c) Ten middle finger fingerprint images. (d) Ten ring finger fingerprint images. (e) Ten little finger fingerprint images.

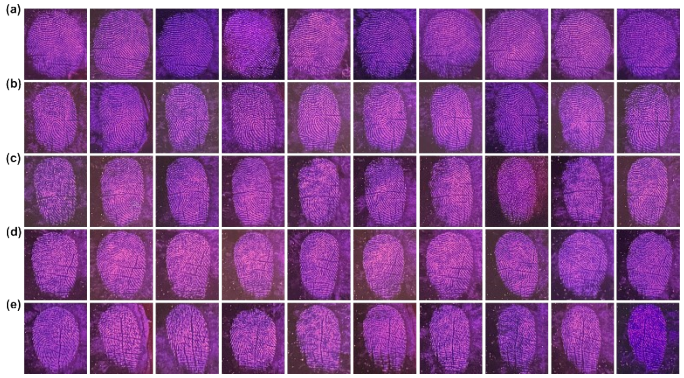

Figure S35. The fingerprint images developed by Eu@**1** from the right hand of volunteer 4 (suspect 4) in the fingerprint database used for training in Alexnet: (a) Ten thumbprint images. (b) Ten index finger fingerprint images. (c) Ten middle finger fingerprint images. (d) Ten ring finger fingerprint images. (e) Ten little finger fingerprint images.

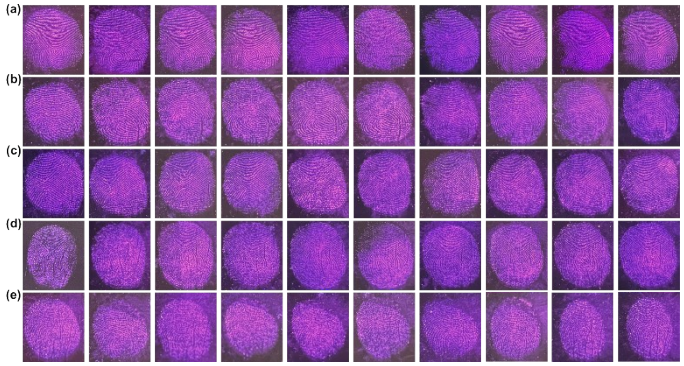

Figure S36. The fingerprint images developed by Eu@**1** from the right hand of volunteer 5 (suspect 5) in the fingerprint database used for training in Alexnet: (a) Ten thumbprint images. (b) Ten index finger fingerprint images. (c) Ten middle finger fingerprint images. (d) Ten ring finger fingerprint images. (e) Ten little finger fingerprint images.

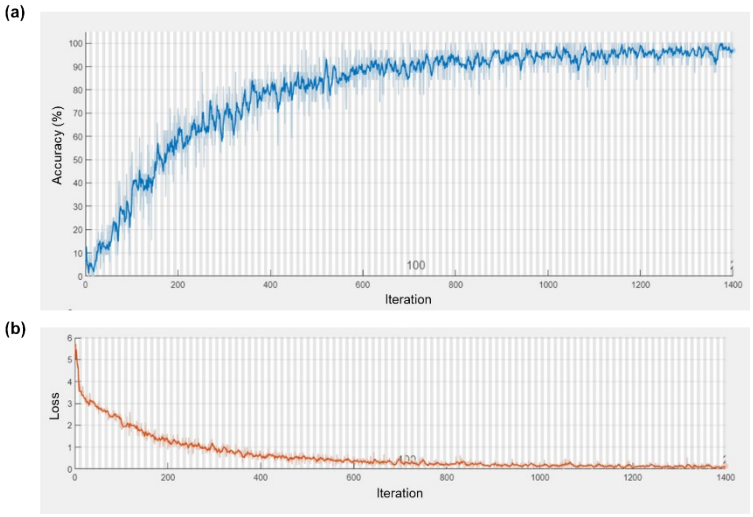

Figure S37. (a) Accuracy training curve of Alexnet neural network after 1400 iterations. (b) Loss training curve of Alexnet neural network after 1400 iterations.

Table S1. Element contents of C and O in EDX energy spectrum of **1** and C, O and Eu in EDS energy spectrum of Eu@**1**.

Element	Weight percentages (%)		Atomic percentage (%)	
	1	Eu@**1**	**1**	Eu@**1**
C	90.54	85.36	92.73	92.17
O	9.46	9.07	7.27	7.36
Eu	-	5.57	-	0.48
Total	100	100	100	100

Table S2. Summary of fluorescence decay lifetime for Eu@**1** powder, Eu@**1** in 90% ethanol, Eu@**1** with 1×10^{-4} M - 5×10^{-4} M Rox, Eu@**1** with 1×10^{-4} M - 5×10^{-4} M AA.

Sample	λ_{ex} (nm)	λ_{em} (nm)	τ_1 (μs)	A_1	Percentage (%)	χ^2
Eu@**1** powder	310	614	573.05	3209.20	100.00	1.590
Eu@**1** in 90% ethanol	324	614	613.30	996.31	100.00	1.447
Eu@**1** with 5×10^{-4} M Rox	324	614	582.03	981.39	100.00	1.700
Eu@**1** with 2×10^{-4} M Rox	324	614	587.74	1097.93	100.00	1.391
Eu@**1** with 1×10^{-4} M Rox	324	614	599.93	1103.70	100.00	1.424
Eu@**1** with 5×10^{-4} M AA	336	614	571.28	507.48	100.00	1.902
Eu@**1** with 2×10^{-4} M AA	330	614	590.13	904.66	100.00	1.425
Eu@**1** with 1×10^{-4} M AA	328	614	600.57	1045.09	100.00	1.515

Table S3. Summary of S_1 and T_1 energy levels (eV) of tcpb calculated by the time dependent density functional theory (TD-DFT) method.

	tcpb
Optimized molecular structure	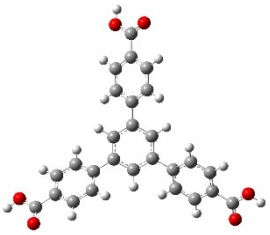
S_1	3.9633 eV
T_1	2.3641 eV

Table S4. Summary of excitation and emission transitions, and experimental energy gaps of tcpb, **1** and Eu^{3+}.

	Transitions	Wavelength (nm)	Energy gap (eV)
tcpb	$S_0 \rightarrow S_n$	346	3.58
	$S_1 \rightarrow S_0$	418	2.97
1	$S_0 \rightarrow S_n$	358	3.46
	$S_1 \rightarrow S_0$	414	3.00
Eu^{3+}	$^5D_0 \rightarrow {}^7F_0$	578	2.15
	$^5D_0 \rightarrow {}^7F_1$	590	2.10
	$^5D_0 \rightarrow {}^7F_2$	614	2.02
	$^5D_0 \rightarrow {}^7F_3$	652	1.90
	$^5D_0 \rightarrow {}^7F_4$	698	1.78

Energy = 1240/λ (eV)

Table S5. Summary of input and output information during the training for SVM.

Input														Output
Rox	AA	Bep	Ani	Sty	Dic	Ben	Nap	Phe	AsO_2	Ara	Hya	Met	Dia	U/Q Infor.
513	-	-	-	-	-	-	-	-	-	-	-	-	-	0
-	35	-	-	-	-	-	-	-	-	-	-	-	-	0
-	-	9184	-	-	-	-	-	-	-	-	-	-	-	1
-	-	-	9301	-	-	-	-	-	-	-	-	-	-	1
-	-	-	-	9315	-	-	-	-	-	-	-	-	-	1
-	-	-	-	-	9508	-	-	-	-	-	-	-	-	1
-	-	-	-	-	-	9777	-	-	-	-	-	-	-	1
-	-	-	-	-	-	-	9806	-	-	-	-	-	-	1
-	-	-	-	-	-	-	-	9967	-	-	-	-	-	1
-	-	-	-	-	-	-	-	-	9640	-	-	-	-	1
-	-	-	-	-	-	-	-	-	-	9170	-	-	-	1
-	-	-	-	-	-	-	-	-	-	-	9230	-	-	1
-	-	-	-	-	-	-	-	-	-	-	-	10068	-	1
-	-	-	-	-	-	-	-	-	-	-	-	-	9714	1

In Table S5, all data is applied to train for the SVM. The fluorescence intensity at 614nm ($^5D_0 \rightarrow {}^7F_2$ transition) of Eu**@1** after response to 14 aromatic and arsenic-containing carcinogens are inputted in the input column of the SVM. Various “0” and “1” are outputted in the output column of the SVM, in which “0” signifies “quenched fluorescence response”, and “1” represents “unchanged fluorescence response”. All data is utilized to train through the SVM.

Table S6. Training result information for SVM.

Training result information	
SVM Type	c_svc
K.F. Type	rbf
γ	0.0714286
Nr_Class	2
Total_SV	14
Rho	-0.714286
Label	1, -1
Nr_SV	12, 2

Support Vector (SV)														
0.710137327	1: -1	2: -1	3: 0.9	4: -1	5: -1	6: -1	7: -1	8: -1	9: -1	10: -1	11: -1	12: -1	13: -1	14: -1
0.710137327	1: -1	2: -1	3: -1	4: 0.9	5: -1	6: -1	7: -1	8: -1	9: -1	10: -1	11: -1	12: -1	13: -1	14: -1
0.707713651	1: -1	2: -1	3: -1	4: -1	5: 0.9	6: -1	7: -1	8: -1	9: -1	10: -1	11: -1	12: -1	13: -1	14: -1
0.707713651	1: -1	2: -1	3: -1	4: -1	5: -1	6:0.9	7: -1	8: -1	9: -1	10: -1	11: -1	12: -1	13: -1	14: -1
0.710137327	1: -1	2: -1	3: -1	4: -1	5: -1	6: -1	7: 0.9	8: -1	9: -1	10: -1	11: -1	12: -1	13: -1	14: -1
0.710137327	1: -1	2: -1	3: -1	4: -1	5: -1	6: -1	7: -1	8: 0.9	9: -1	10: -1	11: -1	12: -1	13: -1	14: -1
0.707713651	1: -1	2: -1	3: -1	4: -1	5: -1	6: -1	7: -1	8: -1	9: 0.9	10: -1	11: -1	12: -1	13: -1	14: -1
0.707713651	1: -1	2: -1	3: -1	4: -1	5: -1	6: -1	7: -1	8: -1	9: -1	10:0.9	11: -1	12: -1	13: -1	14: -1
0.710137327	1: -1	2: -1	3: -1	4: -1	5: -1	6: -1	7: -1	8: -1	9: -1	10: -1	11:0.9	12: -1	13: -1	14: -1
0.710137327	1: -1	2: -1	3: -1	4: -1	5: -1	6: -1	7: -1	8: -1	9: -1	10: -1	11: -1	12:0.9	13: -1	14: -1
0.710137327	1:-1	2: -1	3: -1	4: -1	5: -1	6: -1	7: -1	8: -1	9: -1	10: -1	11: -1	12: -1	13:0.9	14: -1
0.710137327	1: -1	2: -1	3: -1	4: -1	5: -1	6: -1	7: -1	8: -1	9: -1	10: -1	11: -1	12: -1	13: -1	14:0.9
-4.255976611	1: 0.9	2: -1	3: -1	4: -1	5: -1	6: -1	7: -1	8: -1	9: -1	10: -1	11: -1	12: -1	13: -1	14: -1
-4.255976611	1: -1	2: 0.9	3: -1	4: -1	5: -1	6: -1	7: -1	8: -1	9: -1	10: -1	11: -1	12: -1	13: -1	14: -1

Deviation statistics: accuracy rate		
Listing	All rows	Calculation rows
U/Q Infor.	1	1

Table S7. The value deviation table for SVM.

Input item														U/Q Information		
Rox	AA	Bep	Ani	Sty	Dic	Ben	Nap	Phe	AsO_2	Ara	Hya	Met	Dia	OV	CV	AR (%)
513	-	-	-	-	-	-	-	-	-	-	-	-	-	0	0	100
-	35	-	-	-	-	-	-	-	-	-	-	-	-	0	0	100
-	-	9184	-	-	-	-	-	-	-	-	-	-	-	1	1	100
-	-	-	9301	-	-	-	-	-	-	-	-	-	-	1	1	100
-	-	-	-	9315	-	-	-	-	-	-	-	-	-	1	1	100
-	-	-	-	-	9508	-	-	-	-	-	-	-	-	1	1	100
-	-	-	-	-	-	9777	-	-	-	-	-	-	-	1	1	100
-	-	-	-	-	-	-	9806	-	-	-	-	-	-	1	1	100
-	-	-	-	-	-	-	-	9967	-	-	-	-	-	1	1	100
-	-	-	-	-	-	-	-	-	9640	-	-	-	-	1	1	100
-	-	-	-	-	-	-	-	-	-	9170	-	-	-	1	1	100
-	-	-	-	-	-	-	-	-	-	-	9230	-	-	1	1	100
-	-	-	-	-	-	-	-	-	-	-	-	10068	-	1	1	100
-	-	-	-	-	-	-	-	-	-	-	-	-	9714	1	1	100

OV: original value, CV: calculated value, AR: accuracy rate.

Table S8. The MATLAB code of the SVM.

MATLAB code

```
function [fO0] = MPredict(fI0, fI1, fI2, fI3, fI4, fI5, fI6, fI7, fI8, fI9, fI10, fI11, fI12, fI13)
    fI0 = (fI0 - (0 + 540 ) / 2.0) /(540 - (0 + 540 ) / 2.0);
    fI1 = (fI1 - (0 + 36.8421052631578974 ) / 2.0) /(36.8421052631578974 - (0 + 36.8421052631578974 ) / 2.0);
    fI2 = (fI2 - (0 + 9667.3684210526316747 ) / 2.0) /(9667.3684210526316747 - (0 + 9667.3684210526316747 ) / 2.0);
    fI3 = (fI3 - (0 + 9790.5263157894733013 ) / 2.0) /(9790.5263157894733013 - (0 + 9790.5263157894733013 ) / 2.0);
    fI4 = (fI4 - (0 + 9805.2631578947366506 ) / 2.0) /(9805.2631578947366506 - (0 + 9805.2631578947366506 ) / 2.0);
    fI5 = (fI5 - (0 + 10008.4210526315800962 ) / 2.0) /(10008.4210526315800962 - (0 + 10008.4210526315800962 ) / 2.0);
    fI6 = (fI6 - (0 + 10291.5789473684217228 ) / 2.0) /(10291.5789473684217228 - (0 + 10291.5789473684217228 ) / 2.0);
    fI7 = (fI7 - (0 + 10322.1052631578950241 ) / 2.0) /(10322.1052631578950241 - (0 + 10322.1052631578950241 ) / 2.0);
    fI8 = (fI8 - (0 + 10491.5789473684217228 ) / 2.0) /(10491.5789473684217228 - (0 + 10491.5789473684217228 ) / 2.0);
    fI9 = (fI9 - (0 + 10147.3684210526316747 ) / 2.0) /(10147.3684210526316747 - (0 + 10147.3684210526316747 ) / 2.0);
    fI10 = (fI10 - (0 + 9652.6315789473683253 ) / 2.0) /(9652.6315789473683253 - (0 + 9652.6315789473683253 ) / 2.0);
    fI11 = (fI11 - (0 + 9715.7894736842117709 ) / 2.0) /(9715.7894736842117709 - (0 + 9715.7894736842117709 ) / 2.0);
    fI12 = (fI12 - (0 + 10597.8947368421049759 ) / 2.0) /(10597.8947368421049759 - (0 + 10597.8947368421049759 ) / 2.0);
```

```
fI13 = (fI13 - (0 + 10225.2631578947366506 ) / 2.0) /(10225.2631578947366506 - (0 + 10225.2631578947366506 ) / 2.0);
fIns =[fI0 fI1 fI2 fI3 fI4 fI5 fI6 fI7 fI8 fI9 fI10 fI11 fI12 fI13];
fCoefs = [0.710137327390315, 0.710137327390315, 0.7077136505050241, 0.7077136505050241, 0.7101373273903152, 0.7101373273903152, 0.707713650505024, 0.707713650505024, 0.7101373273903153, 0.7101373273903153, 0.7101373273903149, 0.7101373273903149, -4.2559766105713077, -4.2559766105713077];
fSVs = [-1, -1, 0.9, -1, -1, -1, -1, -1, -1, -1, -1, -1, -1; -1, -1, -1, 0.9, -1, -1, -1, -1, -1, -1, -1, -1, -1; -1, -1, -1, -1, 0.9, -1, -1, -1, -1, -1, -1, -1, -1; -1, -1, -1, -1, -1, 0.9, -1, -1, -1, -1, -1, -1, -1; -1, -1, -1, -1, -1, -1, 0.9, -1, -1, -1, -1, -1, -1; -1, -1, -1, -1, -1, 0.9, -1, -1, -1, -1, -1, -1, -1; -1, -1, -1, 0.9, -1, -1, -1, -1, -1; -1, -1, -1, -1, -1, -1, -1, -1, 0.9, -1, -1, -1, -1; -1, -1, -1, -1, -1, -1, -1, -1, -1, 0.9, -1, -1, -1; -1, -1, -1, -1, -1, -1, -1, -1, -1, -1, 0.9, -1, -1; -1, -1, -1, -1, -1, -1, -1, -1, -1, -1, -1, -1, 0.9; 0.9, -1, -1, -1, -1, -1, -1, -1, -1, -1, -1, -1, -1; -1, 0.9, -1, -1, -1, -1, -1, -1, -1, -1, -1, -1, -1];
fRhos = [-0.7142857142857136];
fKVals = [0 0 0 0 0 0 0 0 0 0 0 0 0 0];
for nI = 1 : 14
fSVI = fSVs(nI,:);
for nJ = 1 :14
fI = fIns(nJ) - fSVI(nJ);
fKVals(nI) = fKVals(nI) + fI * fI;
end
fKI = fKVals(nI);
fKVals(nI) = exp(-0.0714285714285714 * fKI);
end
nNRClass = 2;
nL = 14;
nStarts = [0 12];
nVotes = [0 0];
nSVs = [12 2];
fDecVals = [0];
nLabs = [1 -1];
nP = 1;
for nI = 1 : 2
for nJ = nI + 1 : 2
fSum = 0;
nSI = nStarts(nI);
nSJ = nStarts(nJ);
nCI = nSVs(nI);
nCJ = nSVs(nJ);
for nK = 1 : nCI
fSum = fSum + fCoefs(nJ -1, nSI + nK) * fKVals(nSI + nK);
end
for nK = 1 : nCJ
fSum = fSum + fCoefs(nI, nSJ + nK) * fKVals(nSJ + nK);
end
fSum = fSum - fRhos(nP);
```

```
fDecVals(nP) = fSum;
if (fDecVals(nP) > 0)
nVotes(nI) = nVotes(nI) + 1;
else
nVotes(nJ) = nVotes(nJ) + 1;
end
nP = nP + 1;
end
end
nIdx = 1;
for nI = 1 + 1 : 2
if (nVotes(nI) > nVotes(nIdx))
nIdx = nI;
end
end
fO0 = nLabs(nIdx);
fO0 = fO0 * (1 - (0 + 1 ) / 2.0) + (0 + 1) / 2.0;
```

Table S9. Summary of fluorescence sensing parameters of Eu@**1** for detecting Rox, AA, Rox in chicken, Rox in egg-white, and AA in serum.

Drug	Concentration range (mol L^{-1})	Linear relationship	R^2	Detection limit (mg L^{-1})
Rox	5×10^{-5} - 1×10^{-3}	y = -7804.2 x – 22944	0.9919	0.2833
AA	1×10^{-5} - 2×10^{-4}	y = -5176.7 x – 18029	0.9912	0.1003
Rox in chicken	8×10^{-5} - 1×10^{-3}	y = -5321 x – 15906	0.9965	0.6827
Rox in egg-white	8×10^{-5} - 1×10^{-3}	y = -5285.8 x – 15343	0.9932	0.4058
AA in serum	1×10^{-5} - 1×10^{-3}	y = -3963.1 x – 14126	0.9905	0.1574

Table S10. Comparison of the proposed method in this work with some previously similar reported methods for Rox and AA detection.

Analyte	method	Material	LOD (mg L^{-1})	Linear range (mol/L)	Ref
Rox	Fluorescenc	Eu@HOF-BTB	0.2833	5.0×10^{-5} – 1.0×10^{-3}	This work
	Fluorescenc	HNU-62	1.1837	0 – 2.0×10^{-5}	1
	LC-HG-AFS	-	0.2000	7.6×10^{-7} – 1.5×10^{-5}	2
AA	Fluorescenc	Eu@HOF-BTB	0.1003	1.0×10^{-5} – 2.0×10^{-4}	This work
	Fluorescenc	Lys-AuNCs	1.2889	3.8×10^{-5} – 3.0×10^{-3}	3
	Fluorescenc	BSA-AuNCs	0.0800	3.8×10^{-7} – 4.9×10^{-5}	4
	Fluorescenc	LMOF	0.2683	0 – 5.0×10^{-5}	5

LC-HG-AFS: liquid chromatography-hydride generation online coupled with atomic fluorescence spectrometry, Lys-AuNCs: lysozyme-functionalized Au nanoclusters, BSA-AuNCs: bovine serum albumin-stabilized gold nanoclusters, LMOF: $Zn_3(TCPTAPE)(H_2O)_2(OH)_2$.

Table S11. The MATLAB code of AFIS.

MATLAB code
function varargout = zwsb2(varargin)
gui_Singleton = 1;
gui_State = struct('gui_Name', mfilename, ...
'gui_Singleton', gui_Singleton, ...
'gui_OpeningFcn', @zwsb2_OpeningFcn, ...
'gui_OutputFcn', @zwsb2_OutputFcn, ...
'gui_LayoutFcn', [] , ...
'gui_Callback', []);
if nargin && ischar(varargin{1})
gui_State.gui_Callback = str2func(varargin{1});
end
if nargout
[varargout{1:nargout}] = gui_mainfcn(gui_State, varargin{:});
else
gui_mainfcn(gui_State, varargin{:});
end
function zwsb2_OpeningFcn(hObject, eventdata, handles, varargin)
handles.output = hObject;
guidata(hObject, handles);
function varargout = zwsb2_OutputFcn(hObject, eventdata, handles)
varargout{1} = handles.output;
function togglebutton1_Callback(hObject, eventdata, handles)
clear all;
close all;

```
clc;
global im1;
[filename,pathname]=uigetfile({'*.*';'*.bmp';'*.jpg';'*.tif';'*.jpg'},'Select Image 1');
if isequal(filename,0)||isequal(pathname,0)
errordlg('You haven't selected a image yet！ ','Tips');
return;
else
image=[pathname,filename];
im1=imread(image);
[h,w,~] = size(im1);
if h~=256
im1 = imresize(im1,[256,256]);
end
end
global im2;
[filename,pathname]=uigetfile({'*.*';'*.bmp';'*.jpg';'*.tif';'*.jpg'},'Select Image 2');
if isequal(filename,0)||isequal(pathname,0)
errordlg('You haven't selected a image yet！ ','Tips');
return;
else
image=[pathname,filename];
im2=imread(image);
[h,w,~] = size(im2);
if h~=256
im2 = imresize(im2,[256,256]);
end
end
f1=double(im1)/255;
g1=double(im2)/255;
Img = f1;
if ndims(Img) == 3
f2 =rgb2gray(Img);
else
f2 = Img;
end
Img = g1;
if ndims(Img) == 3
g2 =rgb2gray(Img);
else
g2 = Img;
end
f3 =imgcut(f2);
g3 =imgcut(g2);
f4 = medfilt2 (f3);
```

```
g4 = medfilt2 (g3);
f5 = imgbin (f4);
g5 = imgbin (g4);
f6 = imgthi (f5);
g6 = imgthi (g5);
f7 = imgpoi (f6);
g7 = imgpoi (g6);
R = imgcom (f7,g7);
imgres (R);
imgplot (f1,f2,f3,f4,f5,f6,f7,g1,g2,g3,g4,g5,g6,g7);
```

Table S12. The MATLAB code of AlexNet-FAP.

MATLAB code for training for fingerprint images in fingerprint library

```
path1 = 'FingerPrintData/train3';
path2 = 'FingerPrintData/test_final';
imdsTrain = imageDatastore(path1, ...
'IncludeSubfolders',true, ...
'LabelSource','foldernames');
imdsValidation = imageDatastore(path2, ...
'IncludeSubfolders',true, ...
'LabelSource','foldernames');
numTrainImages = numel(imdsTrain.Labels);
numClasses = numel(categories(imdsTrain.Labels));
fprintf('Training sample %d,Total %d \n', numTrainImages, numClasses);
net = alexnet;
inputSize = net.Layers(1).InputSize;
layerTransfer = net.Layers(1:end-3);
layers = [layerTransfer
fullyConnectedLayer(numClasses)
softmaxLayer
classificationLayer];
imageAugmenter = imageDataAugmenter( ...
'FillValue',0, ...
'RandXReflection', 1.5,...
'RandYReflection', 1.5,...
'RandRotation', [-5,10],...
'RandXScale', [0.8,1.2],...
'RandYScale', [0.8,1.2],...
'RandXShear', [-5,5],...
'RandYShear', [-5,5],...
'RandXTranslation',[-5,5], ...
'RandYTranslation',[-5,5]);
augimdsTrain = augmentedImageDatastore([227,227],imdsTrain, 'DataAugmentation',imageAugmenter');
augimdsValidation = augmentedImageDatastore([227,227],imdsValidation);
```

```
minibatch = preview(augimdsTrain);
figure;imshow(imtile(minibatch.input));
options = trainingOptions('sgdm', ...
MiniBatchSize',32, ...
MaxEpochs',200, ...
InitialLearnRate',1e-4, ...
'Shuffle','every-epoch', ...
'Verbose',false, ...
'Plots','training-progress');
netTransfer = trainNetwork(augimdsTrain,layers,options);
save(strcat('model.mat'),'netTransfer')
path2 = 'FingerPrintData/test_final/';
imdsValidation = imageDatastore(path2, ...
'IncludeSubfolders',true, ...
'LabelSource','foldernames');
augimdsValidation = augmentedImageDatastore([227,227],imdsValidation);
load(strcat('model.mat'),'netTransfer')
[YPred,scores] = classify(netTransfer,augimdsValidation);
YValidation = imdsValidation.Labels;
figure
cfsmat = confusionmat(YValidation,YPred);
confusionchart(YValidation,YPred)
acc = sum((YPred) == imdsValidation.Labels)/length(YPred);
fprintf('Classification ended with an accuracy rate of %s \n', num2str(acc) );
```

MATLAB code for texting actual fingerprint images

```
clear
clc
close all
imds = imageDatastore('FingerPrintData/test_final', ...
'IncludeSubfolders',true, ...
'LabelSource','foldernames');
[file,path] = uigetfile("FingerPrintData\test_final\*.png");
I = imread([path,'/',file]);
img = imresize(I,[227,227]);
load(strcat('model.mat'),'netTransfer')
[YPred,scores] = classify(netTransfer,img);
clas = split(path,'\');
truth = categorical(cellstr(clas{end-1}));
if ~exist('result/True/','dir')
mkdir('result/True/')
end
if ~exist('result/False/','dir')
mkdir('result/False/')
end
```

```
if YPred == truth
savepath = fullfile('result/True/',file);
disp('Identificate correctly, and check the result folder')
else
savepath = fullfile('result/False/',file);
disp('Identificate wrongly,and check the result folder')
end
imwrite(I,savepath);
figure(9)
imshow(I);title(YPred)
```

Reference

[1] C. Wang, G. Ren, Q. Tan, G. Che, J. Luo, M. Li, Q. Zhou, D.-Y. Guo, Q. Pan, *Spectrochim. Acta. A Mol. Biomol. Spectrosc.* **2023**, 299, 122812.

[2] J. Liu, H. Yu, H. Song, J. Qiu, F. Sun, P. Li, S. Yang, *J. Environ. Monit.* **2008**, 10, 975-978.

[3] S.-Q. Wu, K.-P. Yin, Y. Sun, Y.-Q. Su, H. Yang, L.-W. Qi, J. Peng, P. L, *Sens. Actuators B Chem.* **2021**, 340,129792.

[4] Y. Lu, Y. Guo, X. Liang, H. Huang, X. Ling, Z. Su, Y. Liang, *Anal. Methods* **2022**, 14, 1963-1972.

[5] C.-R. Guo, Y.-M. Ying, M. Yu, Y. Xiong, X.-G. Liu, Z. Zhao, *ACS Omega* **2021**, 6, 2177-2183.